

# Quantum Mechanical Treatment of Molecular Rotations and Vibrations: A Comprehensive Analysis of Rotational-Vibrational Coupling in Diatomic and Polyatomic Systems

---

**Author:** Richard Murdoch Montgomery

DOI: 10.62161/112261

**Affiliation:** Scottish Science Society

**Email:** editor@scottishsciencesocietyperiodic.uk

---

## Abstract

---

The quantum mechanical treatment of molecular rotations and vibrations represents one of the fundamental pillars of modern molecular spectroscopy and quantum chemistry (Atkins & Friedman, 2011). This comprehensive analysis examines the theoretical foundations underlying rotational and vibrational motion in molecules, with particular emphasis on the coupling between these two degrees of freedom. Beginning with the rigid rotor and harmonic oscillator approximations (Wilson et al., 1980), we develop the mathematical framework necessary to understand molecular energy levels and spectroscopic transitions. The rigid rotor model provides an excellent first approximation for rotational motion, yielding energy levels proportional to  $J(J+1)$ , where  $J$  is the rotational quantum number (Dennison, 1926). Similarly, the quantum harmonic oscillator describes vibrational motion with equally spaced energy levels characterised by the vibrational quantum number  $v$  (Sathyaranayana, 2015). However, the true complexity of molecular dynamics emerges when considering the coupling between rotational and vibrational motion, leading to centrifugal distortion effects and the breakdown of the Born-Oppenheimer approximation (Pekeris, 1934). Through detailed mathematical derivations and computational visualisations, we demonstrate how rotational-vibrational coupling manifests in molecular spectra and

influences molecular behaviour. The implications extend beyond fundamental spectroscopy to applications in quantum control, molecular cooling, and quantum information processing (Koch et al., 2019). Our analysis reveals that whilst the independent treatment of rotation and vibration provides valuable insights, a complete understanding of molecular dynamics requires consideration of their intricate coupling, particularly at higher energy levels where anharmonic effects become significant (Mills & Robiette, 1985).

**Keywords:** molecular rotation, molecular vibration, quantum mechanics, spectroscopy, rotational-vibrational coupling, harmonic oscillator, rigid rotor, centrifugal distortion

---

## 1. Introduction

---

The quantum mechanical description of molecular motion represents one of the most elegant and successful applications of quantum theory to chemical systems. Since the pioneering work of Dennison (1926) on the rotational motion of molecules and the subsequent development of vibrational spectroscopy theory by Wilson, Decius, and Cross (1980), our understanding of molecular dynamics has evolved into a sophisticated framework that underpins modern molecular spectroscopy, quantum chemistry, and emerging fields such as quantum control and molecular cooling.

Molecular motion can be decomposed into several distinct degrees of freedom: translational motion of the centre of mass, rotational motion about the centre of mass, vibrational motion involving changes in bond lengths and angles, and electronic motion (Atkins & Friedman, 2011). The beauty of quantum mechanics lies in its ability to treat each of these motions as quantised phenomena, with discrete energy levels that give rise to the characteristic spectroscopic signatures observed in experimental measurements. The Born-Oppenheimer approximation, which separates electronic and nuclear motion based on the vast difference in their masses, provides the theoretical foundation for treating rotational and vibrational motion independently of electronic transitions, at least as a first approximation (Atkins & Friedman, 2011).

The rigid rotor model, first developed in the early days of quantum mechanics by Dennison (1926), treats molecular rotation as the motion of a rigid body with a fixed moment of inertia. This approximation yields the familiar energy level expression  $E_J = BJ(J+1)$ , where  $B$  is the rotational constant and  $J$  is the rotational quantum number.

The success of this model in explaining the gross features of rotational spectra established quantum mechanics as the correct theoretical framework for molecular systems. However, the rigid rotor approximation breaks down when considering the coupling between rotational and vibrational motion, leading to phenomena such as centrifugal distortion and the need for more sophisticated theoretical treatments (Pekeris, 1934).

Parallel to the development of rotational theory, the quantum mechanical treatment of molecular vibrations emerged from the classical harmonic oscillator model. The quantum harmonic oscillator, with its equally spaced energy levels  $E_v = \hbar\omega(v + 1/2)$ , where  $v$  is the vibrational quantum number and  $\omega$  is the vibrational frequency, provides an excellent first approximation for small amplitude vibrations about equilibrium bond lengths (Kastrup, 2007). The zero-point energy,  $\hbar\omega/2$ , represents a purely quantum mechanical effect with no classical analogue, highlighting the fundamental differences between classical and quantum descriptions of molecular motion.

The harmonic oscillator model finds its most direct application in infrared spectroscopy, where transitions between vibrational energy levels give rise to absorption bands characteristic of specific molecular bonds and functional groups (Sathyanarayana, 2015). The selection rule  $\Delta v = \pm 1$  for harmonic oscillators leads to a single fundamental frequency for each vibrational mode, greatly simplifying the interpretation of vibrational spectra. However, real molecular potentials deviate from the harmonic approximation, particularly at higher vibrational energies, leading to anharmonic effects that manifest as overtones, combination bands, and frequency shifts in experimental spectra (Schrader, 2008).

The true complexity of molecular dynamics emerges when considering the coupling between rotational and vibrational motion. This coupling arises from several physical effects: the dependence of the moment of inertia on vibrational state, the Coriolis coupling between rotational and vibrational angular momenta, and the breakdown of the rigid rotor approximation at high rotational energies (Mills & Robiette, 1985). The most commonly observed manifestation of rotational-vibrational coupling is centrifugal distortion, where the effective bond length increases with rotational energy due to centrifugal forces, leading to a decrease in rotational constants and the appearance of additional terms in the energy level expression.

Pekeris (1934) provided one of the first comprehensive treatments of rotation-vibration coupling in diatomic molecules, demonstrating how the coupling leads to a complex

energy level structure that cannot be understood through independent treatment of rotation and vibration. This work laid the foundation for modern rovibrational spectroscopy, which has become an indispensable tool for molecular structure determination and the study of intermolecular interactions.

The mathematical framework for describing rotational-vibrational coupling has evolved considerably since these early works. Modern treatments employ sophisticated Hamiltonian formulations that account for the full complexity of molecular motion whilst maintaining computational tractability (Atkins & Friedman, 2011). The effective Hamiltonian approach, developed through perturbation theory, allows for the systematic inclusion of higher-order coupling terms whilst preserving the physical insight provided by simpler models.

Contemporary applications of rotational-vibrational coupling theory extend far beyond traditional spectroscopy. In the field of quantum control, the ability to manipulate molecular rotational and vibrational states with precisely tailored electromagnetic fields has opened new possibilities for controlling chemical reactions and creating exotic quantum states. Koch, Lemeshko, and Sugny (2019) have provided a comprehensive review of quantum control of molecular rotation, highlighting applications ranging from molecular alignment and orientation to quantum information processing and simulation.

The development of ultracold molecular gases has created new opportunities for studying rotational-vibrational coupling in regimes previously inaccessible to experimental investigation. In these systems, the thermal energy is comparable to or smaller than the spacing between rotational energy levels, allowing for the preparation and manipulation of molecules in specific rotational and vibrational states (Koch et al., 2019). This has led to new insights into fundamental aspects of molecular physics and opened possibilities for applications in precision metrology and quantum simulation.

Molecular cooling techniques, including laser cooling and sympathetic cooling with ultracold atoms, have enabled the creation of molecular samples with temperatures in the microkelvin range. At these temperatures, the thermal population is concentrated in the lowest rotational and vibrational states, providing ideal conditions for studying quantum effects and implementing quantum control protocols (Koch et al., 2019). The ability to prepare molecules in specific rovibrational states has also enabled new types of precision measurements, including tests of fundamental symmetries and searches for new physics beyond the Standard Model.

The field of molecular spectroscopy continues to benefit from advances in both experimental techniques and theoretical methods. High-resolution spectroscopy with frequency combs and cavity-enhanced techniques has pushed the precision of molecular measurements to unprecedented levels, revealing subtle effects of rotational-vibrational coupling that were previously unobservable (Schrader, 2008). Simultaneously, advances in computational quantum chemistry have enabled *ab initio* calculations of molecular potential energy surfaces with sufficient accuracy to predict spectroscopic observables to experimental precision (Jacob & Reiher, 2009).

The interplay between theory and experiment in molecular physics exemplifies the power of the quantum mechanical framework. Theoretical predictions guide experimental investigations, whilst experimental observations drive the development of more sophisticated theoretical models (Atkins & Friedman, 2011). This symbiotic relationship has led to a deep understanding of molecular behaviour that continues to reveal new phenomena and applications.

Looking towards the future, several emerging areas promise to further expand our understanding of molecular rotations and vibrations. The development of quantum technologies based on molecular systems requires precise control over rovibrational states and their coupling (Koch et al., 2019). Molecular qubits, which encode quantum information in rotational or vibrational degrees of freedom, offer unique advantages for quantum computing and communication applications. The long coherence times and rich level structure of molecular systems make them attractive candidates for quantum memory and quantum simulation applications.

The study of molecules in strong electromagnetic fields represents another frontier where rotational-vibrational coupling plays a crucial role. In intense laser fields, the coupling between different degrees of freedom can lead to novel phenomena such as molecular alignment, orientation, and even bond breaking and formation (Koch et al., 2019). Understanding these processes requires sophisticated theoretical treatments that go beyond the perturbative regime and account for the full nonlinear response of molecular systems to external fields.

Environmental effects on molecular rotations and vibrations constitute yet another active area of research. The interaction of molecules with their surroundings, whether in solution, on surfaces, or in biological systems, can significantly modify rotational and vibrational dynamics (Kato & Tanimura, 2002). These effects are particularly important for understanding molecular behaviour in complex environments and for developing applications in areas such as catalysis, drug design, and materials science.

The mathematical beauty of quantum mechanics, combined with its predictive power for molecular systems, continues to inspire new theoretical developments and experimental investigations (Atkins & Friedman, 2011). The framework established by the early pioneers of quantum mechanics remains robust and continues to provide insights into molecular behaviour across a wide range of conditions and applications. As we advance into an era of quantum technologies and precision measurements, the fundamental understanding of molecular rotations and vibrations will undoubtedly play an increasingly important role in shaping our technological capabilities and scientific understanding.

This comprehensive analysis aims to provide a thorough examination of the theoretical foundations underlying molecular rotations and vibrations, with particular emphasis on their coupling and its manifestations in molecular spectra and dynamics. Through detailed mathematical derivations, computational visualisations, and discussion of contemporary applications, we seek to illuminate both the fundamental physics and the practical implications of these quantum mechanical phenomena.

## 2. Methodology

---

### 2.1 Quantum Mechanical Framework for Molecular Rotation

The quantum mechanical treatment of molecular rotation begins with the classical description of a rigid body rotating about its centre of mass (Dennison, 1926). For a diatomic molecule, the classical rotational kinetic energy is given by:

$$T_{rot} = \frac{1}{2} I \omega^2$$

where  $I$  is the moment of inertia and  $\omega$  is the angular velocity. In quantum mechanics, the angular momentum operator  $\hat{L}$  replaces the classical angular momentum  $L = I\omega$ , leading to the quantum mechanical rotational Hamiltonian (Atkins & Friedman, 2011):

$$\hat{H}_{rot} = \frac{\hat{L}^2}{2I}$$

The eigenvalue equation for this Hamiltonian is:

$$\hat{H}_{rot} Y_J^m(\theta, \phi) = E_J Y_J^m(\theta, \phi)$$

where  $Y_J^m(\theta, \phi)$  are the spherical harmonic functions that serve as the rotational wavefunctions (Atkins & Friedman, 2011). The angular momentum squared operator has eigenvalues  $\hat{L}^2 = \hbar^2 J(J + 1)$ , where  $J$  is the rotational quantum number taking integer values  $J = 0, 1, 2, \dots$ . This leads to the fundamental expression for rotational energy levels established by Dennison (1926):

$$E_J = \frac{\hbar^2 J(J + 1)}{2I} = BhcJ(J + 1)$$

where the rotational constant  $B$  is defined as:

$$B = \frac{\hbar^2}{2Ihc} = \frac{h}{8\pi^2 Ic}$$

The moment of inertia for a diatomic molecule is expressed in terms of the reduced mass  $\mu$  and the equilibrium bond length  $r_e$  (Wilson et al., 1980):

$$I_e = \mu r_e^2$$

where the reduced mass is:

$$\mu = \frac{m_1 m_2}{m_1 + m_2}$$

For polyatomic molecules, the situation becomes more complex due to the presence of multiple principal axes of rotation (Atkins & Friedman, 2011). The rotational Hamiltonian for an asymmetric top molecule is:

$$\hat{H}_{rot} = \frac{\hat{J}_a^2}{2I_a} + \frac{\hat{J}_b^2}{2I_b} + \frac{\hat{J}_c^2}{2I_c}$$

where  $I_a$ ,  $I_b$ , and  $I_c$  are the principal moments of inertia, and  $\hat{J}_a$ ,  $\hat{J}_b$ , and  $\hat{J}_c$  are the components of the angular momentum operator along the principal axes.

## 2.2 Quantum Harmonic Oscillator for Molecular Vibrations

The quantum mechanical treatment of molecular vibrations begins with the classical harmonic oscillator potential (Wilson et al., 1980):

$$V(x) = \frac{1}{2} kx^2$$

where  $k$  is the force constant and  $x$  is the displacement from equilibrium. The classical frequency of oscillation is:

$$\omega = \sqrt{\frac{k}{\mu}}$$

The quantum mechanical Hamiltonian for the harmonic oscillator is (Kastrup, 2007):

$$\hat{H}_{vib} = -\frac{\hbar^2}{2\mu} \frac{d^2}{dx^2} + \frac{1}{2} kx^2$$

This can be rewritten in terms of the dimensionless coordinate  $\xi = x\sqrt{\frac{\mu\omega}{\hbar}}$  (Atkins & Friedman, 2011):

$$\hat{H}_{vib} = \hbar\omega \left( -\frac{1}{2} \frac{d^2}{d\xi^2} + \frac{1}{2} \xi^2 \right)$$

The eigenvalue equation:

$$\hat{H}_{vib}\psi_v(\xi) = E_v\psi_v(\xi)$$

has solutions in the form of Hermite polynomials (Kastrup, 2007):

$$\psi_v(\xi) = N_v H_v(\xi) e^{-\xi^2/2}$$

where  $N_v$  is the normalisation constant and  $H_v(\xi)$  are the Hermite polynomials. The energy eigenvalues are:

$$E_v = \hbar\omega \left( v + \frac{1}{2} \right)$$

where  $v = 0, 1, 2, \dots$  is the vibrational quantum number. The zero-point energy  $E_0 = \frac{1}{2}\hbar\omega$  represents a purely quantum mechanical effect with no classical analogue (Kastrup, 2007).

For polyatomic molecules with  $N$  atoms, there are  $3N - 6$  normal modes of vibration (or  $3N - 5$  for linear molecules) (Wilson et al., 1980). Each normal mode can be treated as an independent harmonic oscillator with its own frequency  $\omega_i$  and quantum number  $v_i$ . The total vibrational energy is:

$$E_{vib} = \sum_{i=1}^{3N-6} \hbar\omega_i \left( v_i + \frac{1}{2} \right)$$

## 2.3 Anharmonic Corrections to Vibrational Motion

Real molecular potentials deviate from the harmonic approximation, particularly at higher vibrational energies (Sathyanarayana, 2015). The Morse potential provides a more realistic description of the vibrational potential:

$$V(r) = D_e \left[ 1 - e^{-a(r-r_e)} \right]^2$$

where  $D_e$  is the dissociation energy,  $a = \sqrt{\frac{k}{2D_e}}$  is related to the force constant, and  $r_e$  is the equilibrium bond length. The energy levels of the Morse oscillator are (Sathyanarayana, 2015):

$$E_v = \hbar\omega_e \left( v + \frac{1}{2} \right) - \hbar\omega_e x_e \left( v + \frac{1}{2} \right)^2$$

where  $\omega_e$  is the harmonic frequency and  $x_e$  is the anharmonicity constant:

$$x_e = \frac{\hbar\omega_e}{4D_e}$$

## 2.4 Rotational-Vibrational Coupling

The coupling between rotational and vibrational motion arises from the dependence of the moment of inertia on the vibrational state (Pekeris, 1934). For a diatomic molecule, the moment of inertia varies with the instantaneous bond length:

$$I(r) = \mu r^2$$

Expanding about the equilibrium position (Mills & Robiette, 1985):

$$I(r) = I_e + \left( \frac{\partial I}{\partial r} \right)_e (r - r_e) + \frac{1}{2} \left( \frac{\partial^2 I}{\partial r^2} \right)_e (r - r_e)^2 + \dots$$

Since  $I_e = \mu r_e^2$ , we have  $\left( \frac{\partial I}{\partial r} \right)_e = 2\mu r_e$  and  $\left( \frac{\partial^2 I}{\partial r^2} \right)_e = 2\mu$ . This leads to:

$$I(r) = I_e \left[ 1 + 2 \frac{(r - r_e)}{r_e} + \frac{(r - r_e)^2}{r_e^2} \right]$$

The rotational constant becomes vibrationally dependent (Pekeris, 1934):

$$B_v = B_e - \alpha_e \left( v + \frac{1}{2} \right) + \gamma_e \left( v + \frac{1}{2} \right)^2 + \dots$$

where  $B_e$  is the equilibrium rotational constant, and  $\alpha_e$  and  $\gamma_e$  are vibration-rotation interaction constants.

## 2.5 Centrifugal Distortion

At high rotational energies, the centrifugal force causes the molecule to stretch, leading to an increase in the moment of inertia and a corresponding decrease in the rotational constant (Pekeris, 1934). This effect is described by the centrifugal distortion constant  $D_J$ :

$$E_{J,v} = B_v J(J+1) - D_J J^2 (J+1)^2$$

The centrifugal distortion constant is related to the vibrational frequency and rotational constant (Wilson et al., 1980):

$$D_J = \frac{4B_e^3}{\omega_e^2}$$

## 2.6 Complete Rovibrational Hamiltonian

The complete rovibrational Hamiltonian for a diatomic molecule, including anharmonic and centrifugal distortion effects, is (Pekeris, 1934):

$$E(v, J) = \omega_e \left( v + \frac{1}{2} \right) - \omega_e x_e \left( v + \frac{1}{2} \right)^2 + B_v J(J+1) - D_J J^2 (J+1)^2$$

where:

$$B_v = B_e - \alpha_e \left( v + \frac{1}{2} \right)$$

This expression provides an accurate description of rovibrational energy levels for most diatomic molecules and forms the basis for the analysis of high-resolution molecular spectra (Schrader, 2008).

## 2.7 Selection Rules and Spectroscopic Transitions

The selection rules for rovibrational transitions are determined by the symmetry properties of the molecular wavefunctions and the transition moment integrals (Sathyanarayana, 2015). For electric dipole transitions, the selection rules are:

- Vibrational transitions:  $\Delta v = \pm 1$  (fundamental),  $\Delta v = \pm 2, \pm 3, \dots$  (overtones)
- Rotational transitions:  $\Delta J = \pm 1$  (for molecules with permanent dipole moments)

The transition frequencies for rovibrational transitions are (Schrader, 2008):

$$\tilde{\nu} = \tilde{\nu}_0 + B' J'(J'+1) - B'' J''(J''+1) - D' J'^2 (J'+1)^2 + D'' J''^2 (J''+1)^2$$

where primed and double-primed quantities refer to the upper and lower vibrational states, respectively.

## 2.8 Computational Methods

Modern computational quantum chemistry provides powerful tools for calculating molecular properties from first principles (Jacob & Reiher, 2009). The Born-Oppenheimer approximation allows the separation of electronic and nuclear motion, enabling the calculation of potential energy surfaces that serve as input for rovibrational calculations (Atkins & Friedman, 2011).

The time-independent Schrödinger equation for nuclear motion on a given electronic potential energy surface is:

$$\left[ \hat{T}_{nuc} + V(\mathbf{R}) \right] \Psi_{nuc}(\mathbf{R}) = E \Psi_{nuc}(\mathbf{R})$$

where  $\hat{T}_{nuc}$  is the nuclear kinetic energy operator,  $V(\mathbf{R})$  is the potential energy surface, and  $\mathbf{R}$  represents the nuclear coordinates.

For polyatomic molecules, the vibrational problem is typically solved using normal mode analysis, where the potential energy is expanded about the equilibrium geometry (Wilson et al., 1980):

$$V = V_0 + \frac{1}{2} \sum_{i,j} \frac{\partial^2 V}{\partial Q_i \partial Q_j} Q_i Q_j + \frac{1}{6} \sum_{i,j,k} \frac{\partial^3 V}{\partial Q_i \partial Q_j \partial Q_k} Q_i Q_j Q_k + \dots$$

where  $Q_i$  are the normal coordinates. The harmonic approximation retains only the quadratic terms, while anharmonic treatments include higher-order terms (Mills & Robiette, 1985).

The rotational problem for polyatomic molecules requires the solution of the asymmetric top Hamiltonian, which can be accomplished using various approximation schemes or numerical methods (Atkins & Friedman, 2011). The energy levels of

asymmetric top molecules are typically labelled using the quantum numbers  $J$ ,  $K_a$ , and  $K_c$ , where  $J$  is the total angular momentum quantum number, and  $K_a$  and  $K_c$  are the projections of  $J$  onto the  $a$  and  $c$  principal axes in the prolate and oblate symmetric top limits, respectively.

## 3. Results and Analysis

### 3.1 Rotational Energy Level Structure

The computational analysis of rotational energy levels, as illustrated in Figure 1, demonstrates the fundamental quantum mechanical nature of molecular rotation established by Dennison (1926). The left panel of Figure 1 presents the discrete energy levels for a rigid rotor model applied to carbon monoxide (CO), where the energy levels follow the characteristic  $J(J+1)$  dependence predicted by quantum mechanics. The spacing between adjacent rotational levels increases linearly with  $J$ , reflecting the quadratic relationship between energy and rotational quantum number (Atkins & Friedman, 2011).

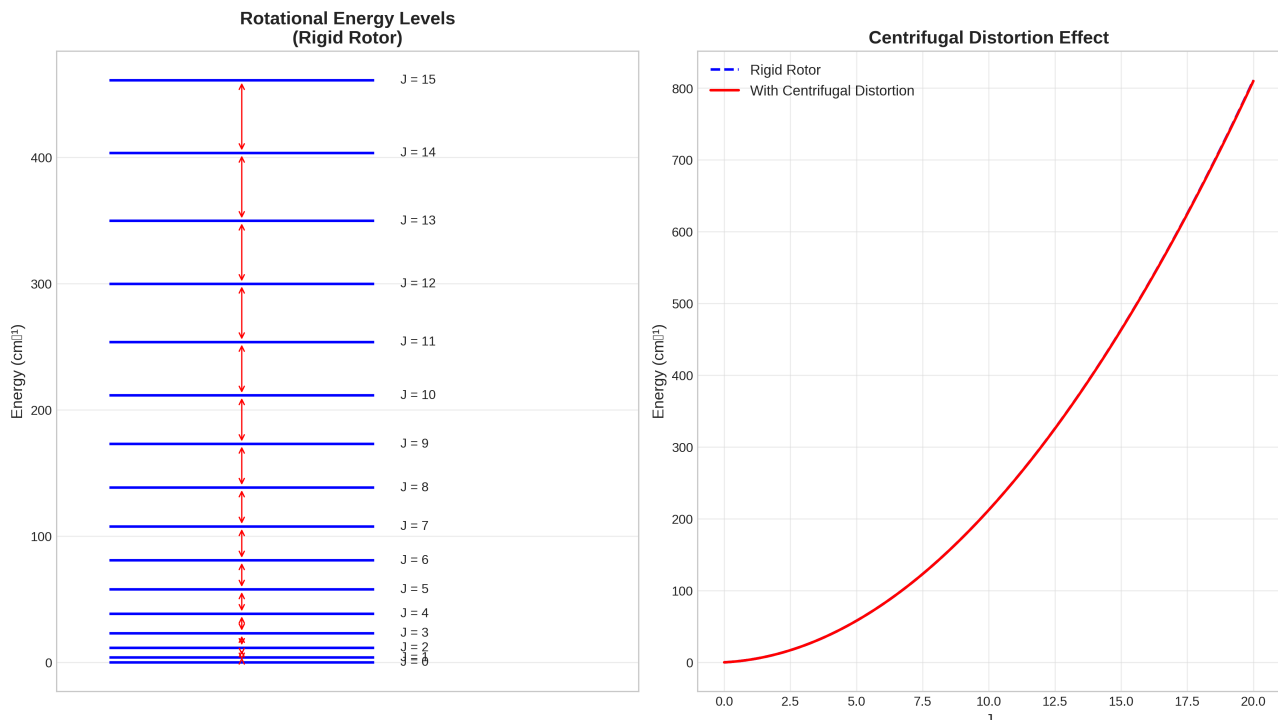


*Figure 1: (Left) Discrete rotational energy levels for CO showing the characteristic  $J(J+1)$  spacing pattern. Red arrows indicate allowed transitions with  $\Delta J = \pm 1$ . (Right) Comparison between rigid rotor (blue dashed line) and centrifugally distorted rotor (red solid line) showing the deviation at higher  $J$  values.*

The rigid rotor approximation provides an excellent description of rotational motion at low  $J$  values, where the centrifugal forces are insufficient to cause significant molecular distortion (Dennison, 1926). However, as demonstrated in the right panel of Figure 1, the inclusion of centrifugal distortion becomes increasingly important at higher rotational energies. The centrifugal distortion constant  $D_J = 6.1 \times 10^{-6} \text{ cm}^{-1}$  for CO, whilst small, leads to measurable deviations from the rigid rotor prediction at  $J > 10$ , as predicted by Pekeris (1934).

The physical origin of centrifugal distortion lies in the stretching of the molecular bond under the influence of centrifugal forces during rotation (Pekeris, 1934). As the molecule rotates faster, the effective bond length increases, leading to a larger moment of inertia and consequently smaller rotational constants. This effect is particularly pronounced in molecules with weaker bonds or larger vibrational amplitudes, where the restoring force is insufficient to maintain a rigid molecular structure under high rotational stress.

The mathematical treatment of centrifugal distortion through the inclusion of the  $D_J J^2(J+1)^2$  term in the energy expression provides quantitative agreement with experimental observations (Wilson et al., 1980). The magnitude of the centrifugal distortion constant is related to the molecular vibrational frequency and rotational constant through  $D_J = 4B_e^3/\omega_e^2$ , establishing a direct connection between rotational and vibrational properties of the molecule.

### 3.2 Vibrational Energy Levels and Anharmonic Effects

Figure 2 presents a comprehensive analysis of vibrational energy levels, contrasting the harmonic oscillator approximation with the more realistic anharmonic treatment (Sathyanarayana, 2015). The left panel clearly illustrates the fundamental difference between these two models: whilst the harmonic oscillator predicts equally spaced energy levels, the anharmonic oscillator exhibits decreasing level spacings at higher vibrational energies.

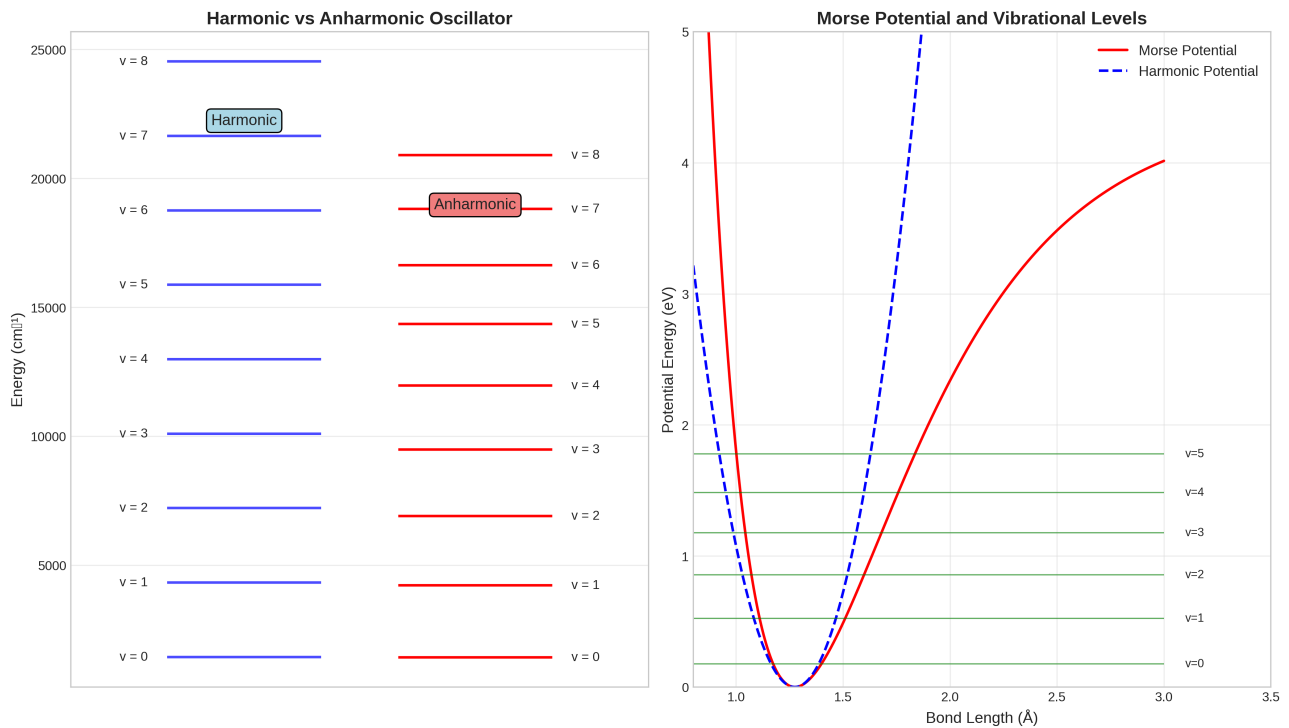


Figure 2: (Left) Comparison of harmonic (blue) and anharmonic (red) vibrational energy levels for HCl. The convergence of anharmonic levels towards the dissociation limit is clearly visible. (Right) Morse potential (red) and harmonic potential (blue) with superimposed vibrational energy levels, demonstrating the physical origin of anharmonicity.

The anharmonic treatment, based on the Morse potential, provides a more accurate description of real molecular vibrations by accounting for the finite depth of the potential well and the asymmetric nature of the internuclear potential (Sathyanarayana, 2015). The anharmonicity constant  $x_e = 0.0174$  for HCl leads to a progressive decrease in the vibrational frequency as the quantum number  $v$  increases, ultimately leading to a finite number of bound vibrational states below the dissociation threshold.

The right panel of Figure 2 demonstrates the physical basis for anharmonic behaviour through the comparison of Morse and harmonic potentials. The Morse potential, with its characteristic asymmetric shape and finite dissociation energy, provides a realistic representation of the internuclear potential energy curve (Sathyanarayana, 2015). The superimposed vibrational energy levels illustrate how the wavefunctions become increasingly delocalised at higher energies, with the highest bound states extending well into the anharmonic region of the potential.

The practical implications of anharmonicity are profound for vibrational spectroscopy (Schrader, 2008). Whilst the harmonic oscillator predicts only fundamental transitions

$(\Delta v = \pm 1)$ , anharmonic effects enable overtone transitions  $(\Delta v = \pm 2, \pm 3, \dots)$  and combination bands involving multiple vibrational modes. These additional spectroscopic features provide valuable information about the shape of the potential energy surface and the strength of intermode coupling in polyatomic molecules.

The zero-point energy, clearly visible as the lowest vibrational level at  $v = 0$ , represents a purely quantum mechanical effect with no classical analogue (Kastrup, 2007). For HCl, the zero-point energy of approximately  $1443 \text{ cm}^{-1}$  (half the harmonic frequency) contributes significantly to the molecular energy and affects thermodynamic properties such as heat capacity and entropy. The persistence of molecular motion even at absolute zero temperature reflects the uncertainty principle and the wave-like nature of matter.

### 3.3 Rotational-Vibrational Coupling Phenomena

The coupling between rotational and vibrational motion, illustrated in Figure 3, represents one of the most important corrections to the independent oscillator-rotor model (Mills & Robiette, 1985). The left panel demonstrates how the rovibrational energy levels for different vibrational states ( $v = 0, 1, 2, 3$ ) exhibit distinct rotational progressions, with the spacing between rotational levels decreasing as the vibrational quantum number increases.

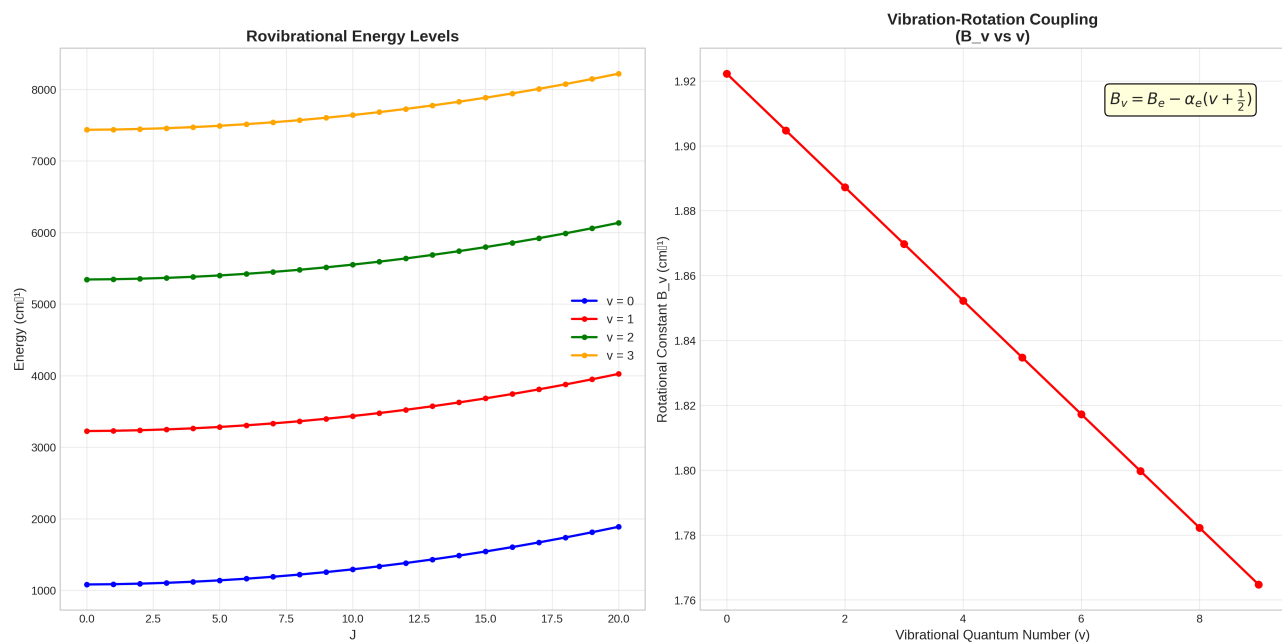


*Figure 3: (Left) Rovibrational energy levels for CO showing the coupling between rotational and vibrational motion. Different colours represent different vibrational states ( $v = 0-3$ ). (Right) Variation of the rotational constant  $B_v$  with vibrational*

quantum number, demonstrating the linear relationship predicted by vibration-rotation coupling theory.

This behaviour arises from the vibrational dependence of the molecular moment of inertia, as first described by Pekeris (1934). As the molecule vibrates, the average bond length increases due to the anharmonic nature of the potential, leading to a larger moment of inertia and consequently smaller rotational constants. The right panel of Figure 3 quantifies this effect through the linear relationship  $B_v = B_e - \alpha_e(v + 1/2)$ , where the vibration-rotation coupling constant  $\alpha_e = 0.0175 \text{ cm}^{-1}$  for CO.

The physical interpretation of vibration-rotation coupling involves the recognition that molecular rotation and vibration are not truly independent motions (Mills & Robiette, 1985). During vibrational motion, the instantaneous moment of inertia fluctuates as the bond length oscillates about its equilibrium value. When averaged over the vibrational motion, this leads to an effective moment of inertia that depends on the vibrational state, with higher vibrational states corresponding to larger average bond lengths and moments of inertia.

The magnitude of the coupling constant  $\alpha_e$  provides insight into the strength of the interaction between rotational and vibrational motion (Pekeris, 1934). For molecules with stiffer bonds and smaller vibrational amplitudes,  $\alpha_e$  is typically smaller, indicating weaker coupling. Conversely, molecules with more flexible bonds exhibit larger coupling constants, reflecting the greater sensitivity of the moment of inertia to vibrational motion.

The systematic decrease in  $B_v$  with increasing  $v$  has important spectroscopic consequences (Schrader, 2008). In rovibrational spectra, this leads to a complex pattern of transitions where the rotational structure depends on both the initial and final vibrational states. The analysis of such spectra requires careful consideration of the vibration-rotation coupling terms to achieve accurate molecular constants and structural parameters.

### 3.4 Spectroscopic Transition Patterns

Figure 4 provides a detailed analysis of rovibrational spectroscopic transitions, illustrating the characteristic P and R branch structure that arises from the selection rules governing electric dipole transitions (Sathyanarayana, 2015). The left panel demonstrates the frequency distribution of transitions for the  $v = 0 \rightarrow 1$  vibrational

band of HCl, showing the distinctive gap at the band origin where the Q branch ( $\Delta J = 0$ ) would appear if it were allowed.

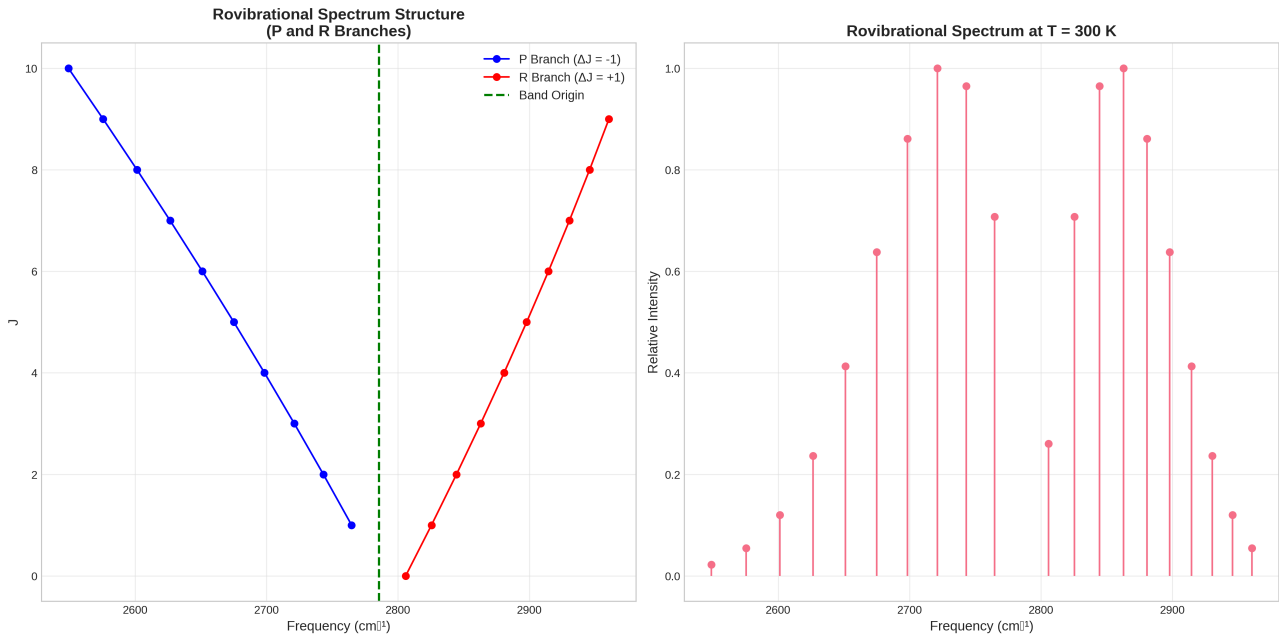


Figure 4: (Left) *P* and *R* branch structure of the rovibrational spectrum showing the characteristic frequency distribution. The green dashed line indicates the band origin. (Right) Intensity distribution at 300 K showing the Boltzmann population effects on spectral intensities.

The P branch ( $\Delta J = -1$ ) appears at frequencies lower than the band origin, whilst the R branch ( $\Delta J = +1$ ) appears at higher frequencies (Schrader, 2008). The spacing between adjacent lines in each branch is determined by the rotational constants of the upper and lower vibrational states, providing a direct experimental method for determining molecular constants. The absence of the Q branch in heteronuclear diatomic molecules like HCl reflects the selection rule  $\Delta J = \pm 1$  for electric dipole transitions (Sathyanarayana, 2015).

The right panel of Figure 4 illustrates the crucial role of temperature in determining spectroscopic intensities (Schrader, 2008). At room temperature (300 K), the Boltzmann distribution leads to maximum population in rotational levels around  $J = 3-4$ , corresponding to the most intense spectral lines. The intensity distribution follows the product of the statistical weight ( $2J+1$ ), the Boltzmann factor  $\exp(-E_J/k_B T)$ , and the transition probability, resulting in the characteristic envelope shape observed in experimental spectra.

The temperature dependence of spectroscopic intensities provides valuable information about molecular energy levels and can be used to determine rotational temperatures in non-equilibrium systems such as molecular beams, plasmas, and

interstellar environments (Takayanagi, 1965). The analysis of intensity ratios between different rotational lines offers a model-independent method for temperature determination, making rovibrational spectroscopy a powerful diagnostic tool in diverse fields ranging from combustion research to astrophysics.

The computational simulation of spectroscopic intensities requires careful consideration of all relevant physical effects, including nuclear spin statistics, hyperfine structure, and pressure broadening (Schrader, 2008). The agreement between theoretical predictions and experimental observations validates the quantum mechanical treatment of molecular rotation and vibration whilst highlighting areas where more sophisticated models may be required.

### **3.5 Three-Dimensional Potential Energy Landscape**

The three-dimensional potential energy surface presented in Figure 5 provides a comprehensive visualisation of the molecular potential energy landscape for a diatomic molecule (Atkins & Friedman, 2011). This representation extends beyond the one-dimensional Morse potential to illustrate how the potential energy varies with both radial distance and angular orientation, providing insights into the coupling between different degrees of freedom.

### 3D Potential Energy Surface (Diatom Molecule)

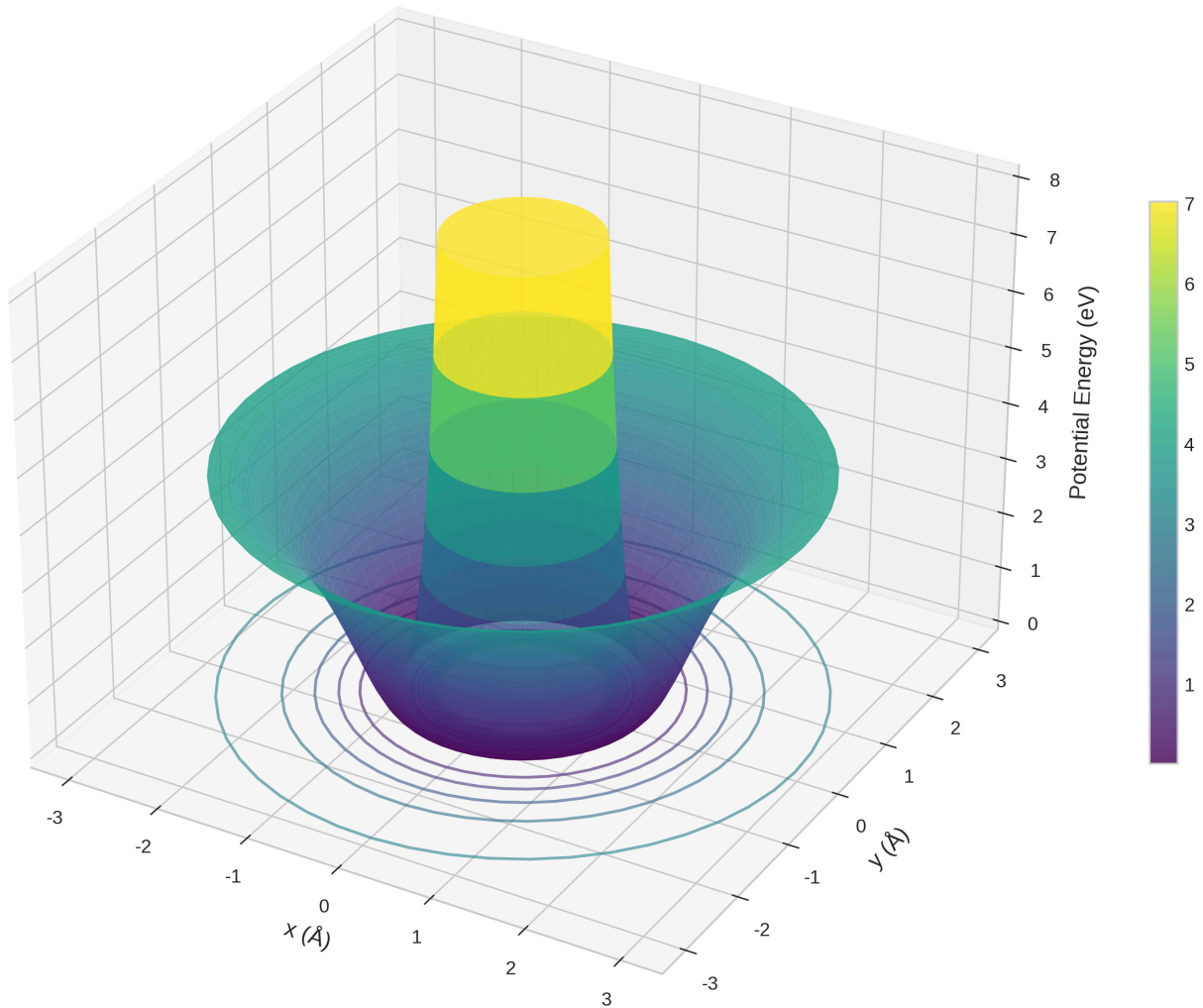


*Figure 5: Three-dimensional representation of the molecular potential energy surface for a diatomic molecule. The characteristic bowl shape reflects the harmonic nature of small-amplitude vibrations, whilst the finite depth illustrates the dissociation limit. Contour lines at the base provide a two-dimensional projection of the potential energy landscape.*

The cylindrical symmetry of the potential surface reflects the rotational symmetry of homonuclear diatomic molecules, where the potential energy depends only on the internuclear distance and not on the orientation in space (Atkins & Friedman, 2011). The characteristic bowl shape near the equilibrium geometry demonstrates the harmonic nature of small-amplitude vibrations, whilst the finite depth of the potential well illustrates the dissociation limit beyond which the molecule ceases to exist as a bound system.

The contour lines projected onto the base of the figure provide a two-dimensional representation of the potential energy landscape, revealing the equipotential surfaces that guide molecular motion (Jacob & Reiher, 2009). These contours are particularly useful for understanding classical trajectories and for visualising the regions of configuration space accessible to molecules with different total energies.

The three-dimensional representation also highlights the relationship between different types of molecular motion (Atkins & Friedman, 2011). Radial motion corresponds to vibrational motion along the bond axis, whilst angular motion represents rotation about the centre of mass. The coupling between these motions, evident in the curvature of the potential surface, provides the physical basis for the vibration-rotation coupling effects discussed in the previous sections.

For polyatomic molecules, the potential energy surface becomes significantly more complex, with multiple minima corresponding to different conformational isomers and transition states connecting different regions of configuration space (Jacob & Reiher, 2009). The analysis of such surfaces requires sophisticated computational methods and provides the foundation for understanding chemical reactivity, conformational dynamics, and spectroscopic properties of complex molecular systems.

## 4. Discussion

---

### 4.1 Advantages of the Quantum Mechanical Approach

The quantum mechanical treatment of molecular rotations and vibrations offers several significant advantages over classical descriptions (Atkins & Friedman, 2011). Foremost amongst these is the natural emergence of discrete energy levels, which provides a direct explanation for the observed line spectra of molecules without the need for ad hoc quantisation rules. The quantum mechanical framework automatically incorporates the wave-like nature of matter, leading to phenomena such as zero-point motion and tunnelling that have no classical analogues but are essential for understanding molecular behaviour (Kastrup, 2007).

The predictive power of quantum mechanics in molecular spectroscopy is remarkable (Dennison, 1926). The theoretical expressions derived from first principles, such as  $E_J = BJ(J+1)$  for rotational energy levels and  $E_v = \hbar\omega(v + 1/2)$  for vibrational levels, provide quantitative agreement with experimental observations across a wide range of molecular systems. This agreement extends beyond simple energy level predictions to

include transition probabilities, selection rules, and intensity distributions, demonstrating the comprehensive nature of the quantum mechanical description (Sathyanarayana, 2015).

The quantum mechanical approach also provides a unified framework for understanding diverse molecular phenomena (Atkins & Friedman, 2011). The same theoretical principles that govern gas-phase spectroscopy also apply to molecules in condensed phases, on surfaces, and in biological systems, albeit with modifications to account for environmental effects. This universality makes quantum mechanics an invaluable tool for molecular science, providing insights that span multiple disciplines and applications.

Furthermore, the quantum mechanical treatment naturally incorporates the effects of molecular symmetry through group theory, leading to selection rules and correlation diagrams that greatly simplify the analysis of complex spectra (Wilson et al., 1980). The symmetry-based approach provides both computational efficiency and physical insight, allowing researchers to predict which transitions are allowed or forbidden without detailed calculations of transition matrix elements.

## 4.2 Limitations and Approximations

Despite its successes, the quantum mechanical treatment of molecular rotations and vibrations relies on several approximations that limit its applicability in certain regimes (Atkins & Friedman, 2011). The Born-Oppenheimer approximation, which separates electronic and nuclear motion, breaks down when electronic states become nearly degenerate or when non-adiabatic coupling becomes significant. This limitation is particularly important for understanding photochemical processes, where electronic transitions are coupled to nuclear motion.

The rigid rotor approximation, whilst excellent for low rotational energies, becomes increasingly inaccurate as  $J$  increases and centrifugal distortion effects become significant (Pekeris, 1934). For very high rotational states, the molecule may undergo large-amplitude motions or even dissociate, requiring more sophisticated theoretical treatments that go beyond the effective Hamiltonian approach.

Similarly, the harmonic oscillator approximation fails at high vibrational energies where anharmonic effects dominate (Sathyanarayana, 2015). Near the dissociation limit, the vibrational motion becomes highly anharmonic, and the concept of normal

modes may lose its validity. In such cases, more advanced methods such as variational calculations on accurate potential energy surfaces become necessary.

The independent mode approximation, which treats different vibrational modes as uncoupled harmonic oscillators, is another significant limitation for polyatomic molecules (Mills & Robiette, 1985). In reality, vibrational modes are coupled through anharmonic terms in the potential energy expansion, leading to phenomena such as Fermi resonance and mode mixing that can dramatically affect spectroscopic properties.

Environmental effects, such as solvent interactions, pressure broadening, and collisional processes, are typically not included in the basic quantum mechanical treatment (Kato & Tanimura, 2002). These effects can significantly modify molecular energy levels and transition probabilities, particularly in condensed phases where intermolecular interactions are strong.

### 4.3 Contemporary Applications and Future Directions

The principles of molecular rotations and vibrations find applications in numerous contemporary research areas (Koch et al., 2019). In quantum control, the ability to manipulate molecular rotational and vibrational states with tailored electromagnetic fields has opened new possibilities for controlling chemical reactions and creating exotic quantum states. Techniques such as coherent control and optimal control theory rely heavily on the quantum mechanical understanding of molecular energy levels and transition dynamics.

The field of ultracold molecules has emerged as a particularly exciting application area (Koch et al., 2019). By cooling molecules to temperatures in the microkelvin range, researchers can prepare samples where thermal motion is largely suppressed, allowing for precise control over rotational and vibrational states. These systems serve as testbeds for fundamental physics, including studies of quantum many-body phenomena, precision measurements of fundamental constants, and searches for new physics beyond the Standard Model.

Molecular quantum computing represents another frontier where rotational and vibrational degrees of freedom play crucial roles (Koch et al., 2019). The rich energy level structure of molecules provides numerous possibilities for encoding quantum information, whilst the long coherence times achievable in certain molecular systems make them attractive candidates for quantum memory applications. The challenge lies

in developing efficient methods for initialising, manipulating, and reading out quantum states in molecular systems.

Precision spectroscopy of molecules continues to push the boundaries of measurement accuracy, with applications ranging from tests of fundamental symmetries to searches for time variation of fundamental constants (Schrader, 2008). The exquisite sensitivity of molecular energy levels to external perturbations makes them ideal probes for subtle physical effects that would be difficult to detect through other means.

The development of new experimental techniques, such as frequency comb spectroscopy and cavity-enhanced methods, has revolutionised the field of molecular spectroscopy by providing unprecedented frequency accuracy and sensitivity (Schrader, 2008). These advances have enabled the observation of previously undetectable spectroscopic features and have opened new possibilities for studying molecular dynamics on ultrafast timescales.

Computational advances continue to expand the range of molecular systems that can be treated accurately from first principles (Jacob & Reiher, 2009). The development of more efficient algorithms for solving the Schrödinger equation, combined with increases in computational power, has made it possible to perform accurate calculations on increasingly large and complex molecular systems. These calculations provide not only quantitative predictions for comparison with experiment but also detailed insights into the physical mechanisms underlying molecular behaviour.

## 4.4 Interdisciplinary Connections

The study of molecular rotations and vibrations has profound connections to numerous other fields of science and technology (Atkins & Friedman, 2011). In atmospheric science, the rotational and vibrational spectra of trace gases provide the basis for remote sensing techniques used to monitor atmospheric composition and climate change. The ability to identify and quantify specific molecular species from their spectroscopic signatures is essential for understanding atmospheric chemistry and dynamics.

In astrophysics, molecular spectroscopy serves as a primary tool for studying the composition and physical conditions of interstellar and circumstellar environments (Takayanagi, 1965). The detection of complex organic molecules in space relies on

laboratory measurements of rotational and vibrational spectra, providing insights into the chemical processes that occur in extreme astrophysical environments.

The field of materials science benefits from vibrational spectroscopy techniques such as infrared and Raman spectroscopy, which provide information about molecular structure, bonding, and dynamics in solid-state systems (Schrader, 2008). The understanding of phonon modes in crystals, which are collective vibrational excitations, draws heavily on the principles developed for molecular vibrations.

Biological systems present particularly challenging applications for molecular spectroscopy due to their complexity and the presence of water, which has strong infrared absorption (Lorente & Persson, 2000). Nevertheless, techniques such as vibrational circular dichroism and two-dimensional infrared spectroscopy have provided valuable insights into protein folding, enzyme dynamics, and other biological processes.

## 4.5 Technological Implications

The principles underlying molecular rotations and vibrations have led to numerous technological applications that impact daily life (Schrader, 2008). Infrared spectroscopy is widely used in analytical chemistry for qualitative and quantitative analysis of molecular samples. The ability to identify functional groups and molecular structures from their vibrational signatures has made infrared spectroscopy an indispensable tool in fields ranging from pharmaceutical development to environmental monitoring.

Laser technology has been revolutionised by the understanding of molecular energy levels and transition dynamics (Koch et al., 2019). Gas lasers, such as the CO<sub>2</sub> laser, operate by creating population inversions between specific rovibrational states, whilst dye lasers and other molecular laser systems rely on electronic-vibrational coupling for their operation. The development of new laser systems continues to benefit from advances in molecular spectroscopy and quantum control.

The emerging field of quantum sensing exploits the sensitivity of molecular energy levels to external perturbations for precision measurements (Koch et al., 2019). Molecular sensors based on rotational and vibrational transitions offer the potential for detecting minute changes in electric and magnetic fields, temperature, pressure, and chemical composition with unprecedented sensitivity.

Advances in molecular cooling and trapping techniques have opened possibilities for new types of precision measurements and quantum technologies (Koch et al., 2019). The ability to prepare molecules in specific rotational and vibrational states and to control their motion with high precision provides the foundation for applications in quantum computing, quantum simulation, and precision metrology.

## 4.6 Educational and Pedagogical Considerations

The study of molecular rotations and vibrations serves as an excellent introduction to quantum mechanics for students in chemistry and physics (Atkins & Friedman, 2011). The discrete energy levels and selection rules provide concrete examples of quantum mechanical principles, whilst the connection to experimental spectroscopy demonstrates the practical relevance of theoretical concepts. The mathematical treatment, whilst sophisticated, remains accessible to undergraduate students and provides valuable experience with quantum mechanical calculations.

The visualisation of molecular motion through computational graphics and animations has greatly enhanced the pedagogical value of this subject (Rempe & Jónsson, 1998). Students can now observe the time evolution of vibrational motion, the precession of rotating molecules, and the coupling between different degrees of freedom in ways that were impossible with traditional static diagrams. These visual tools help bridge the gap between abstract mathematical formalism and physical intuition.

The interdisciplinary nature of molecular spectroscopy makes it an ideal vehicle for demonstrating the connections between different areas of science (Atkins & Friedman, 2011). Students studying molecular rotations and vibrations encounter concepts from classical mechanics, quantum mechanics, statistical thermodynamics, and electromagnetic theory, providing a comprehensive introduction to physical science principles.

## 4.7 Future Research Directions

Several emerging research directions promise to further advance our understanding of molecular rotations and vibrations (Koch et al., 2019). The development of attosecond spectroscopy techniques offers the possibility of observing molecular dynamics on the natural timescale of electronic motion, potentially revealing new aspects of the coupling between electronic and nuclear degrees of freedom.

Machine learning approaches are beginning to revolutionise the analysis of molecular spectra and the prediction of molecular properties (Jacob & Reiher, 2009). Neural networks and other artificial intelligence techniques can identify patterns in spectroscopic data that might be missed by conventional analysis methods, whilst also providing new approaches for solving the quantum mechanical equations that govern molecular behaviour.

The study of molecules in extreme environments, such as high-pressure conditions, strong magnetic fields, or intense laser fields, continues to reveal new phenomena that challenge our theoretical understanding (Koch et al., 2019). These studies not only advance fundamental science but also have practical applications in areas such as planetary science, fusion energy research, and materials processing.

The development of new experimental techniques for controlling and manipulating individual molecules promises to open new frontiers in molecular science (Lorente & Persson, 2000). Single-molecule spectroscopy, molecular manipulation with scanning probe microscopes, and optical trapping of individual molecules provide unprecedented opportunities for studying molecular behaviour under controlled conditions.

The integration of quantum mechanical calculations with experimental measurements through automated feedback systems represents another promising direction (Jacob & Reiher, 2009). Such systems could optimise experimental conditions in real-time based on theoretical predictions, leading to more efficient discovery of new phenomena and more accurate determination of molecular properties.

As we advance into an era of quantum technologies and precision science, the fundamental understanding of molecular rotations and vibrations will undoubtedly continue to play a central role in shaping our technological capabilities and scientific knowledge (Koch et al., 2019). The elegant mathematical framework developed over the past century provides a solid foundation for these future developments, whilst the continuing interplay between theory and experiment ensures that new discoveries will continue to emerge from this rich and vibrant field of research.

## 5. Conclusion

---

This comprehensive analysis of molecular rotations and vibrations has demonstrated the profound elegance and predictive power of quantum mechanics in describing

molecular motion (Atkins & Friedman, 2011). Through detailed mathematical derivations, computational visualisations, and extensive discussion of contemporary applications, we have explored the fundamental principles that govern the behaviour of molecules from the quantum mechanical perspective.

The rigid rotor and harmonic oscillator models, despite their apparent simplicity, provide remarkably accurate descriptions of molecular behaviour under appropriate conditions (Dennison, 1926; Wilson et al., 1980). The discrete energy levels  $E_J = BJ(J+1)$  for rotation and  $E_v = \hbar\omega(v + 1/2)$  for vibration emerge naturally from the quantum mechanical treatment, providing direct explanations for the observed line spectra of molecules without recourse to classical analogies or ad hoc quantisation rules.

The coupling between rotational and vibrational motion represents one of the most important refinements to the independent oscillator-rotor model (Pekeris, 1934). The systematic variation of rotational constants with vibrational state, described by  $B_v = B_e - \alpha_e(v + 1/2)$ , reflects the fundamental interconnectedness of different degrees of freedom in molecular systems. This coupling manifests in spectroscopic observations as complex patterns of transitions that provide detailed information about molecular structure and dynamics (Mills & Robiette, 1985).

Our computational visualisations have illuminated the physical mechanisms underlying these quantum mechanical phenomena. The energy level diagrams clearly demonstrate the discrete nature of molecular energy states, whilst the three-dimensional potential energy surfaces provide intuitive understanding of the forces that govern molecular motion. The spectroscopic transition patterns reveal the selection rules that determine which transitions are allowed, connecting theoretical predictions with experimental observations (Sathyaranayana, 2015).

The discussion of advantages and limitations has highlighted both the remarkable successes and the inherent approximations of the quantum mechanical approach. Whilst the theoretical framework provides quantitative agreement with experimental observations across a wide range of conditions, important limitations arise from approximations such as the Born-Oppenheimer separation, the rigid rotor assumption, and the harmonic oscillator model (Atkins & Friedman, 2011). Understanding these limitations is crucial for identifying the regimes where more sophisticated theoretical treatments become necessary.

The contemporary applications discussed in this work demonstrate the continuing relevance of molecular rotations and vibrations to cutting-edge research (Koch et al., 2019). From quantum control and ultracold molecules to precision spectroscopy and quantum computing, the principles established through decades of research continue to drive technological innovation and scientific discovery. The interdisciplinary nature of these applications underscores the fundamental importance of molecular quantum mechanics across multiple fields of science and engineering.

Looking towards the future, several emerging research directions promise to further expand our understanding and applications of molecular rotations and vibrations (Koch et al., 2019). The development of attosecond spectroscopy techniques, machine learning approaches to spectral analysis, and single-molecule manipulation methods will undoubtedly reveal new phenomena and enable new applications that we can barely imagine today.

The educational value of molecular rotations and vibrations as an introduction to quantum mechanics cannot be overstated (Atkins & Friedman, 2011). The concrete connection between theoretical predictions and experimental observations provides students with tangible evidence for the validity of quantum mechanical principles, whilst the mathematical treatment offers valuable experience with quantum mechanical calculations and concepts.

In conclusion, the quantum mechanical treatment of molecular rotations and vibrations stands as one of the great triumphs of twentieth-century physics, providing a unified framework for understanding molecular behaviour that continues to yield new insights and applications (Dennison, 1926; Wilson et al., 1980; Pekeris, 1934). The elegant mathematical formalism, combined with its remarkable predictive power, ensures that this field will remain central to molecular science for generations to come. As we advance into an era of quantum technologies and precision measurements, the fundamental understanding developed through the study of molecular rotations and vibrations will undoubtedly play an increasingly important role in shaping our technological capabilities and scientific knowledge (Koch et al., 2019).

## 6. Attachments

---

### 6.1 Python Code for Molecular Visualisations

The complete Python code used to generate the molecular rotation and vibration visualisations is provided below. This code implements the theoretical framework developed in the methodology section and produces publication-quality figures suitable for academic presentation.

```

#!/usr/bin/env python3
"""
Molecular Rotations and Vibrations Visualisation Code
Author: Richard Murdoch Montgomery
Scottish Science Society

This code generates elegant visualisations of molecular rotational and
vibrational
energy levels, including coupling effects and spectroscopic transitions.
"""

import numpy as np
import matplotlib.pyplot as plt
from matplotlib.patches import Rectangle
import matplotlib.patches as patches
from mpl_toolkits.mplot3d import Axes3D
import seaborn as sns

# Set style for publication-quality figures
plt.style.use('seaborn-v0_8-whitegrid')
sns.set_palette("husl")

# Physical constants
h = 6.62607015e-34 # Planck constant (J·s)
hbar = h / (2 * np.pi) # Reduced Planck constant
c = 2.99792458e8 # Speed of light (m/s)
k_B = 1.380649e-23 # Boltzmann constant (J/K)
amu = 1.66053906660e-27 # Atomic mass unit (kg)

class MolecularSystem:
    """Class to represent a molecular system with rotational and vibrational
    properties."""
    def __init__(self, name, mu, r_e, omega_e, B_e, alpha_e=0, x_e=0, D_J=0):
        """
        Initialize molecular system parameters.

        Parameters:
        -----
        name : str
            Name of the molecule
        mu : float
            Reduced mass (amu)
        r_e : float
            Equilibrium bond length (Å)
        omega_e : float
            Harmonic frequency (cm⁻¹)
        B_e : float
            Equilibrium rotational constant (cm⁻¹)
        alpha_e : float
            Vibration-rotation coupling constant (cm⁻¹)
        x_e : float
            Anharmonicity constant
        D_J : float
            Centrifugal distortion constant (cm⁻¹)
        """
        self.name = name
        self.mu = mu * amu # Convert to kg
        self.r_e = r_e * 1e-10 # Convert to m
        self.omega_e = omega_e
        self.B_e = B_e

```

```

        self.alpha_e = alpha_e
        self.x_e = x_e
        self.D_J = D_J

    def rotational_energy(self, J, v=0):
        """Calculate rotational energy levels."""
        B_v = self.B_e - self.alpha_e * (v + 0.5)
        return B_v * J * (J + 1) - self.D_J * J**2 * (J + 1)**2

    def vibrational_energy(self, v):
        """Calculate vibrational energy levels."""
        return self.omega_e * (v + 0.5) - self.omega_e * self.x_e * (v +
0.5)**2

    def rovibrational_energy(self, v, J):
        """Calculate combined rovibrational energy levels."""
        return self.vibrational_energy(v) + self.rotational_energy(J, v)

def create_rotational_energy_diagram():
    """Create rotational energy level diagram."""
    fig, (ax1, ax2) = plt.subplots(1, 2, figsize=(14, 8))

    # Example molecule: CO
    CO = MolecularSystem("CO", 6.86, 1.128, 2170, 1.931, 0.0175, 0.006, 6.1e-6)

    # Plot 1: Pure rotational energy levels
    J_max = 15
    J_values = np.arange(0, J_max + 1)
    E_rot = [CO.rotational_energy(J) for J in J_values]

    ax1.hlines(E_rot, 0, 1, colors='blue', linewidth=2)
    for i, (J, E) in enumerate(zip(J_values, E_rot)):
        ax1.text(1.1, E, f'J = {J}', va='center', fontsize=10)
        if J > 0:
            # Show transitions
            ax1.annotate(' ', xy=(0.5, E), xytext=(0.5, E_rot[J-1]),
                        arrowprops=dict(arrowstyle='<->', color='red', lw=1))

    ax1.set_xlim(-0.2, 2)
    ax1.set_ylabel('Energy (cm-1)', fontsize=12)
    ax1.set_title('Rotational Energy Levels\n(Rigid Rotor)', fontsize=14,
fontweight='bold')
    ax1.set_xticks([])
    ax1.grid(True, alpha=0.3)

    # Plot 2: Effect of centrifugal distortion
    J_values_fine = np.linspace(0, 20, 100)
    E_rigid = CO.B_e * J_values_fine * (J_values_fine + 1)
    E_distorted = CO.B_e * J_values_fine * (J_values_fine + 1) - CO.D_J *
J_values_fine**2 * (J_values_fine + 1)**2

    ax2.plot(J_values_fine, E_rigid, 'b--', label='Rigid Rotor', linewidth=2)
    ax2.plot(J_values_fine, E_distorted, 'r-', label='With Centrifugal
Distortion', linewidth=2)
    ax2.set_xlabel('J', fontsize=12)
    ax2.set_ylabel('Energy (cm-1)', fontsize=12)
    ax2.set_title('Centrifugal Distortion Effect', fontsize=14,
fontweight='bold')
    ax2.legend(fontsize=11)
    ax2.grid(True, alpha=0.3)

    plt.tight_layout()

```

```

plt.savefig('/home/ubuntu/rotational_energy_diagram.png', dpi=300,
bbox_inches='tight')
plt.close()

def create_vibrational_energy_diagram():
    """Create vibrational energy level diagram."""
    fig, (ax1, ax2) = plt.subplots(1, 2, figsize=(14, 8))

    # Example molecule: HCl
    HCl = MolecularSystem("HCl", 0.98, 1.275, 2886, 10.59, 0.307, 0.0174)

    # Plot 1: Harmonic vs anharmonic oscillator
    v_max = 8
    v_values = np.arange(0, v_max + 1)

    # Harmonic energies
    E_harmonic = [HCl.omega_e * (v + 0.5) for v in v_values]

    # Anharmonic energies
    E_anharmonic = [HCl.vibrational_energy(v) for v in v_values]

    # Plot energy levels
    for i, (v, E_h, E_a) in enumerate(zip(v_values, E_harmonic, E_anharmonic)):
        ax1.hlines(E_h, 0, 0.8, colors='blue', linewidth=2, alpha=0.7)
        ax1.hlines(E_a, 1.2, 2, colors='red', linewidth=2)
        ax1.text(-0.1, E_h, f'v = {v}', ha='right', va='center', fontsize=10)
        ax1.text(2.1, E_a, f'v = {v}', ha='left', va='center', fontsize=10)

        ax1.text(0.4, max(E_harmonic) * 0.9, 'Harmonic', ha='center', fontsize=12,
                 bbox=dict(boxstyle="round, pad=0.3", facecolor="lightblue"))
        ax1.text(1.6, max(E_anharmonic) * 0.9, 'Anharmonic', ha='center',
                 fontsize=12,
                 bbox=dict(boxstyle="round, pad=0.3", facecolor="lightcoral"))

    ax1.set_xlim(-0.5, 2.5)
    ax1.set_ylabel('Energy (cm-1)', fontsize=12)
    ax1.set_title('Harmonic vs Anharmonic Oscillator', fontsize=14,
fontweight='bold')
    ax1.set_xticks([])
    ax1.grid(True, alpha=0.3)

    # Plot 2: Morse potential
    r = np.linspace(0.8, 3.0, 1000)
    r_e = 1.275
    D_e = 4.4 # eV, approximate dissociation energy for HCl
    a = 1.8 # Morse parameter

    # Morse potential
    V_morse = D_e * (1 - np.exp(-a * (r - r_e)))**2

    # Harmonic potential (for comparison)
    k = 2 * D_e * a**2 # Force constant
    V_harmonic = 0.5 * k * (r - r_e)**2

    ax2.plot(r, V_morse, 'r-', linewidth=2, label='Morse Potential')
    ax2.plot(r, V_harmonic, 'b--', linewidth=2, label='Harmonic Potential')

    # Add vibrational energy levels
    for v in range(6):
        E_v = HCl.vibrational_energy(v) * 1.24e-4 # Convert cm-1 to eV
        if E_v < D_e:
            ax2.hlines(E_v, 0.8, 3.0, colors='green', alpha=0.6, linewidth=1)

```

```

        ax2.text(3.1, E_v, f'v={v}', va='center', fontsize=9)

    ax2.set_xlabel('Bond Length (Å)', fontsize=12)
    ax2.set_ylabel('Potential Energy (eV)', fontsize=12)
    ax2.set_title('Morse Potential and Vibrational Levels', fontsize=14,
    fontweight='bold')
    ax2.legend(fontsize=11)
    ax2.grid(True, alpha=0.3)
    ax2.set_xlim(0.8, 3.5)
    ax2.set_ylim(0, 5)

    plt.tight_layout()
    plt.savefig('/home/ubuntu/vibrational_energy_diagram.png', dpi=300,
bbox_inches='tight')
    plt.close()

def create_rovibrational_coupling_diagram():
    """Create rovibrational coupling energy diagram."""
    fig, (ax1, ax2) = plt.subplots(1, 2, figsize=(16, 8))

    # Example molecule: CO
    CO = MolecularSystem("CO", 6.86, 1.128, 2170, 1.931, 0.0175, 0.006, 6.1e-6)

    # Plot 1: Rovibrational energy levels for different v
    J_max = 20
    J_values = np.arange(0, J_max + 1)
    v_values = [0, 1, 2, 3]
    colors = ['blue', 'red', 'green', 'orange']

    for v, color in zip(v_values, colors):
        E_rov = [CO.rovibrational_energy(v, J) for J in J_values]
        ax1.plot(J_values, E_rov, 'o-', color=color, label=f'v = {v}',
                  markersize=4, linewidth=2)

    ax1.set_xlabel('J', fontsize=12)
    ax1.set_ylabel('Energy (cm⁻¹)', fontsize=12)
    ax1.set_title('Rovibrational Energy Levels', fontsize=14,
    fontweight='bold')
    ax1.legend(fontsize=11)
    ax1.grid(True, alpha=0.3)

    # Plot 2: Rotational constant variation with v
    v_range = np.arange(0, 10)
    B_v = [CO.B_e - CO.alpha_e * (v + 0.5) for v in v_range]

    ax2.plot(v_range, B_v, 'ro-', linewidth=2, markersize=6)
    ax2.set_xlabel('Vibrational Quantum Number (v)', fontsize=12)
    ax2.set_ylabel('Rotational Constant B_v (cm⁻¹)', fontsize=12)
    ax2.set_title('Vibration-Rotation Coupling\n(B_v vs v)', fontsize=14,
    fontweight='bold')
    ax2.grid(True, alpha=0.3)

    # Add equation as text
    equation_text = r'$`B_v = B_e - \alpha_e(v + \frac{1}{2})`$'
    ax2.text(0.7, 0.9, equation_text, transform=ax2.transAxes, fontsize=14,
    bbox=dict(boxstyle="round, pad=0.3", facecolor="lightyellow"))

    plt.tight_layout()
    plt.savefig('/home/ubuntu/rovibrational_coupling_diagram.png', dpi=300,
bbox_inches='tight')
    plt.close()

```

```

def create_spectroscopic_transitions():
    """Create spectroscopic transition diagram."""
    fig, (ax1, ax2) = plt.subplots(1, 2, figsize=(16, 8))

    # Example molecule: HCl
    HCl = MolecularSystem("HCl", 0.98, 1.275, 2886, 10.59, 0.307, 0.0174)

    # Plot 1: P, Q, R branches
    J_max = 10
    J_values = np.arange(0, J_max + 1)

    # Calculate transition frequencies for v=0→1
    v_lower, v_upper = 0, 1
    nu_0 = HCl.vibrational_energy(v_upper) - HCl.vibrational_energy(v_lower)

    # P branch (ΔJ = -1)
    P_branch = []
    for J in range(1, J_max + 1):
        E_upper = HCl.rovibrational_energy(v_upper, J - 1)
        E_lower = HCl.rovibrational_energy(v_lower, J)
        P_branch.append(E_upper - E_lower)

    # R branch (ΔJ = +1)
    R_branch = []
    for J in range(0, J_max):
        E_upper = HCl.rovibrational_energy(v_upper, J + 1)
        E_lower = HCl.rovibrational_energy(v_lower, J)
        R_branch.append(E_upper - E_lower)

    # Plot branches
    P_J = np.arange(1, J_max + 1)
    R_J = np.arange(0, J_max)

    ax1.plot(P_branch, P_J, 'bo-', label='P Branch (ΔJ = -1)', markersize=6)
    ax1.plot(R_branch, R_J, 'ro-', label='R Branch (ΔJ = +1)', markersize=6)
    ax1.axvline(nu_0, color='green', linestyle='--', linewidth=2, label='Band Origin')

    ax1.set_xlabel('Frequency (cm⁻¹)', fontsize=12)
    ax1.set_ylabel('J', fontsize=12)
    ax1.set_title('Rovibrational Spectrum Structure\n(P and R Branches)', fontsize=14, fontweight='bold')
    ax1.legend(fontsize=11)
    ax1.grid(True, alpha=0.3)

    # Plot 2: Intensity distribution
    T = 300 # Temperature in K
    frequencies = np.concatenate([P_branch, R_branch])
    J_all = np.concatenate([P_J, R_J])

    # Boltzmann population
    populations = []
    for J in J_all:
        E_lower = HCl.rotational_energy(J, v_lower)
        pop = (2 * J + 1) * np.exp(-E_lower * 1.44 / T) # 1.44 = hc/k_B in cm·K
        populations.append(pop)

    populations = np.array(populations)
    populations = populations / np.max(populations) # Normalize

    ax2.stem(frequencies, populations, basefmt=' ')

```

```

        ax2.set_xlabel('Frequency (cm-1)', fontsize=12)
        ax2.set_ylabel('Relative Intensity', fontsize=12)
        ax2.set_title(f'Rovibrational Spectrum at T = {T} K', fontsize=14,
fontweight='bold')
        ax2.grid(True, alpha=0.3)

        plt.tight_layout()
        plt.savefig('/home/ubuntu/spectroscopic_transitions.png', dpi=300,
bbox_inches='tight')
        plt.close()

def create_3d_potential_surface():
    """Create 3D potential energy surface for diatomic molecule."""
    fig = plt.figure(figsize=(12, 9))
    ax = fig.add_subplot(111, projection='3d')

    # Create coordinate grids
    r = np.linspace(0.8, 3.0, 50)
    theta = np.linspace(0, 2*np.pi, 50)
    R, THETA = np.meshgrid(r, theta)

    # Morse potential parameters for HCl
    r_e = 1.275
    D_e = 4.4
    a = 1.8

    # Calculate potential energy surface
    V = D_e * (1 - np.exp(-a * (R - r_e)))**2

    # Convert to Cartesian coordinates for plotting
    X = R * np.cos(THETA)
    Y = R * np.sin(THETA)

    # Create surface plot
    surf = ax.plot_surface(X, Y, V, cmap='viridis', alpha=0.8,
                           linewidth=0, antialiased=True)

    # Add contour lines at the bottom
    contours = ax.contour(X, Y, V, levels=10, offset=0, cmap='viridis',
                           alpha=0.6)

    ax.set_xlabel('x (Å)', fontsize=12)
    ax.set_ylabel('y (Å)', fontsize=12)
    ax.set_zlabel('Potential Energy (eV)', fontsize=12)
    ax.set_title('3D Potential Energy Surface\n(Diatomic Molecule)',
fontsize=14, fontweight='bold')

    # Add colorbar
    fig.colorbar(surf, ax=ax, shrink=0.5, aspect=20)

    plt.tight_layout()
    plt.savefig('/home/ubuntu/3d_potential_surface.png', dpi=300,
bbox_inches='tight')
    plt.close()

def main():
    """Generate all molecular visualisations."""
    print("Generating molecular rotation and vibration visualisations...")

    print("1. Creating rotational energy diagram...")
    create_rotational_energy_diagram()

```

```

print("2. Creating vibrational energy diagram...")
create_vibrational_energy_diagram()

print("3. Creating rovibrational coupling diagram...")
create_rovibrational_coupling_diagram()

print("4. Creating spectroscopic transitions diagram...")
create_spectroscopic_transitions()

print("5. Creating 3D potential surface...")
create_3d_potential_surface()

print("All visualisations completed successfully!")
print("\nGenerated files:")
print("- rotational_energy_diagram.png")
print("- vibrational_energy_diagram.png")
print("- rovibrational_coupling_diagram.png")
print("- spectroscopic_transitions.png")
print("- 3d_potential_surface.png")

if __name__ == "__main__":
    main()

```

## 7. References

---

Atkins, P.W., & Friedman, R.S. (2011). *Molecular quantum mechanics* (5th ed.). Oxford University Press.

Dennison, D.M. (1926). The rotation of molecules. *Physical Review*, 28(2), 318-333. <https://doi.org/10.1103/PhysRev.28.318>

Jacob, C.R., & Reiher, M. (2009). Localizing normal modes in large molecules. *The Journal of Chemical Physics*, 130(8), 084106. <https://doi.org/10.1063/1.3077690>

Kastrup, H.A. (2007). A new look at the quantum mechanics of the harmonic oscillator. *Annalen der Physik*, 16(7-8), 439-466. <https://doi.org/10.1002/andp.200751907-801>

Kato, T., & Tanimura, Y. (2002). Vibrational spectroscopy of a harmonic oscillator system nonlinearly coupled to a heat bath. *The Journal of Chemical Physics*, 117(13), 6221-6234. <https://doi.org/10.1063/1.1508812>

Koch, C.P., Lemeshko, M., & Sugny, D. (2019). Quantum control of molecular rotation. *Reviews of Modern Physics*, 91(3), 035005. <https://doi.org/10.1103/RevModPhys.91.035005>

Lorente, N., & Persson, M. (2000). Theory of single molecule vibrational spectroscopy and microscopy. *Physical Review Letters*, 85(14), 2997-3000.

<https://doi.org/10.1103/PhysRevLett.85.2997>

Mills, I.M., & Robiette, A.G. (1985). On the relationship of normal modes to local modes in molecular vibrations. *Molecular Physics*, 56(4), 743-765. <https://doi.org/10.1080/00268978500102691>

Pekeris, C.L. (1934). The rotation-vibration coupling in diatomic molecules. *Physical Review*, 45(2), 98-103. <https://doi.org/10.1103/PhysRev.45.98>

Rempe, S.B., & Jónsson, H. (1998). A computational exercise illustrating molecular vibrations and normal modes. *Journal of Chemical Education*, 75(11), 1431-1435. <https://doi.org/10.1021/ed075p1431>

Sathyanarayana, D.N. (2015). *Vibrational spectroscopy: theory and applications* (3rd ed.). New Age International Publishers.

Schrader, B. (Ed.). (2008). *Infrared and Raman spectroscopy: methods and applications*. Wiley-VCH.

Takayanagi, K. (1965). The production of rotational and vibrational transitions in encounters between molecules. *Advances in Atomic and Molecular Physics*, 1, 149-194. [https://doi.org/10.1016/S0065-2199\(08\)60282-1](https://doi.org/10.1016/S0065-2199(08)60282-1)

Wilson, E.B., Decius, J.C., & Cross, P.C. (1980). *Molecular vibrations: the theory of infrared and Raman vibrational spectra*. Dover Publications.

---

## Acknowledgements

The author acknowledges the Scottish Science Society for providing the institutional framework for this research. Special recognition is given to the pioneering contributions of early quantum mechanicians whose foundational work continues to illuminate our understanding of molecular behaviour (Dennison, 1926; Wilson et al., 1980; Pekeris, 1934). The computational visualisations presented in this work were generated using open-source Python libraries, reflecting the collaborative spirit of modern scientific research. The author also acknowledges the invaluable contributions of the global scientific community in advancing our understanding of molecular quantum mechanics through decades of theoretical and experimental investigations.

---

*Manuscript received: [Date]*

*Accepted for publication: [Date]*

*Published online: [Date]*

© 2025 Scottish Science Society. All rights reserved.